

# New brown dwarfs in Upper Sco using UKIDSS Galactic Cluster Survey science verification data <sup>\*</sup>

N. Lodieu<sup>1</sup>† N. C. Hambly<sup>2</sup>, R. F. Jameson<sup>1</sup>, S. T. Hodgkin<sup>3</sup>, G. Carraro<sup>4,5</sup> and T.R. Kendall<sup>6</sup>

<sup>1</sup>*Department of Physics & Astronomy, University of Leicester, University Road, Leicester LE1 7RH, UK*

<sup>2</sup>*Scottish Universities' Physics Alliance (SUPA), Institute for Astronomy, School of Physics, University of Edinburgh, Royal Observatory, Blackford Hill, Edinburgh EH9 3HJ, UK*

<sup>3</sup>*Institute of Astronomy, Madingley Road, Cambridge, CB3 0HA, UK*

<sup>4</sup>*Departamento de Astronomia, Universidad de Chile, Casilla 36-D, Santiago, Chile*

<sup>5</sup>*Astronomy Department, Yale University, PO Box 208101, New Haven, CT 06520-8101, USA*

<sup>6</sup>*Centre for Astrophysics Research, Science & Technology Research Institute, Department of Physics Astronomy & Mathematics, University of Hertfordshire, College Lane, Hatfield, Hertfordshire AL10 9AB*

Accepted —. Received —; in original form —

## ABSTRACT

We present first results from a deep ( $J = 18.7$ ), wide-field (6.5 square degrees) infrared ( $ZYJHK$ ) survey in the Upper Sco association conducted within the science verification phase of the UKIRT Infrared Deep Sky Survey Galactic Cluster Survey (GCS). Cluster members define a sequence well separated from field stars in the ( $Z - J, Z$ ) colour-magnitude diagram. We have selected a total of 164 candidates with  $J = 10.5$ – $18.7$  mag from the ( $Z - J, Z$ ) and ( $Y - J, Y$ ) diagrams. We further investigated the location of those candidates in the other colour-magnitude and colour-colour diagrams to weed out contaminants. The cross-correlation of the GCS catalogue with the 2MASS database confirms the membership of 116 photometric candidates down to 20 Jupiter masses as they lie within a  $2\sigma$  circle centred on the association mean motion. The final list of cluster members contains 129 sources with masses between 0.3 and  $0.007 M_{\odot}$ . We extracted a dozen new low-mass brown dwarfs below  $20 M_{Jup}$ , the limit of previous surveys in the region. Finally, we have derived the mass function in Upper Sco over the 0.3– $0.01 M_{\odot}$  mass range, best fit by a single segment with a slope of index  $\alpha = 0.6 \pm 0.1$ , in agreement with previous determination in open clusters.

**Key words:** Techniques: photometric — Infrared: stars — open clusters and associations: individual: Upper Sco — Stars: low-mass, brown dwarfs — Stars: luminosity function, mass function

## 1 INTRODUCTION

The Scorpius Centaurus is the nearest OB association, located at a distance of  $145 \pm 2$  pc from the Sun (de Bruijne et al. 1997; de Zeeuw et al. 1999). The association spans 120 square degrees and is composed of 3 subgroups: Upper Scorpius, Upper Centaurus Lupus, and Lower Centaurus Crux (Blaauw 1964). The age of the Upper Sco association is about 5 Myr with little scatter (Preibisch & Zinnecker 2002). The region is free of extinc-

tion with  $A_v \leq 2$  mag, suggesting that star formation has already ended (Walter et al. 1994).

The association has been studied at multiple wavelengths over the past decade. Walter et al. (1994) identified 28 low-mass stars over  $7 \text{ deg}^2$  in Upper Sco from an X-ray survey performed with the Einstein satellite. Preibisch et al. (1998) performed a larger scale X-ray survey of 160 square degrees with ROSAT and obtained spectroscopy for selected candidates, suggesting that 39 of them are indeed genuine members of the association. de Bruijne et al. (1997) extracted 115 additional members from trigonometric parallaxes and kinematic information available for a sample of 1215 Hipparcos stars. Preibisch et al. (2001) and Preibisch & Zinnecker (2002) published a sample of spectroscopically confirmed X-ray selected members in the range

<sup>\*</sup> Based on observations made with the United Kingdom Infrared Telescope, operated by the Joint Astronomy Centre on behalf of the U.K. Particle Physics and Astronomy Research Council.

† E-mail: nl41@star.le.ac.uk

2.0 to 0.1  $M_{\odot}$  over 6 square degrees. The derived mass function (not corrected for binaries) is in agreement with the field Initial Mass Function (IMF; Scalo 1998; Kroupa 2002). The hydrogen burning boundary was crossed with the discovery of 64 very low-mass stars and brown dwarfs with spectral types later than M5.5 by independent studies (Ardila et al. 2000; Mohanty et al. 2004; Martín et al. 2004; Slesnick et al. 2006).

The UKIRT Infrared Deep Sky Survey (UKIDSS; Lawrence et al. 2006) constitutes a new generation of deep, large-scale infrared surveys. It consists of 5 components: the Large Area Survey, the Galactic Cluster Survey (hereafter GCS), the Galactic Plane Survey, the Deep Extragalactic Survey, and the Ultra-Deep Survey. The GCS will cover  $\sim 1000$  square degrees in 10 star forming regions and open clusters down to  $K = 18.4$  at two epochs. The main scientific driver of the survey is to study the Initial Mass Function and its dependence with environment in the substellar regime using a uniformly selected data set of low-mass stars and brown dwarfs. Ultimately, the full coverage of the targets and the availability of two epochs for proper motion measurement will provide a complete census of very low-mass stars, brown dwarfs, and planetary mass objects.

In this paper we analyse a 6.5 square degree survey conducted in the Upper Sco association during the Science Verification phase of the UKIDSS project. In Sect. 2 we briefly present the observations, the catalogue products, and the selection of sources. In Sect. 3 we describe the photometric selection of cluster candidates in Upper Sco from various colour-magnitude diagrams and estimate proper motions for the brighter stars using 2MASS (Cutri et al. 2003) to provide first epoch positions. We also discuss possible contamination of our sample and conclude that it will be very small. In Sect. 4 we discuss the main results of the survey, including the mass function down to 10 Jupiter masses. Finally, we give our conclusions in Sect. 5.

## 2 THE UKIDSS GCS IN UPPER SCO

Eight tiles were observed with the UKIRT Wide-Field CAMera (WFCAM) in the association during the Science Verification phase on 2005 April 8–13 covering a total of 6.5 square degrees (Fig. 1) in *ZYJHK* broadband filters (Hewett et al. 2006); details of the filters are given in Table 1. The *Z* WFCAM filter is narrower than optical *z* filters while the *Y* filter was specifically designed to uncover the coolest brown dwarfs and furthest quasars, those being the main scientific goals of the Large Area Survey. In particular, a  $Y - J \geq 1$  selects L and T dwarfs. The WFCAM focal plane array includes 4 Rockwell 2048  $\times$  2048 chips each covering a 13.6 arcmin by 13.6 arcmin field resulting in a non-contiguous ‘pawprint’ with a pixel scale of 0.4 arcsec. Each chip is spaced by  $\sim 95\%$  of the device size implying that four pawprints are required to obtain contiguous coverage in a tile of 0.8 square degrees (Casali et al. 2006, in preparation).

A summary of the observations, including the 8 WFCAM pointings, central coordinates, date of observations, weather conditions, and seeing is provided in Tables 2 and 3. Exposure times were set to 40 seconds in all passbands, yielding 100% detection completeness limits of  $Z = 20.1$ ,

**Table 1.** Central wavelengths, 50% cut-on and 50% cut-off (in microns) for the 5 WFCAM bandpasses.

Passband:	<i>Z</i>	<i>Y</i>	<i>J</i>	<i>H</i>	<i>K</i>
Central wavelength	0.88	1.03	1.25	1.65	2.20
50% cut-on	0.83	0.97	1.17	1.49	2.03
50% cut-off	0.925	1.07	1.33	1.78	2.37

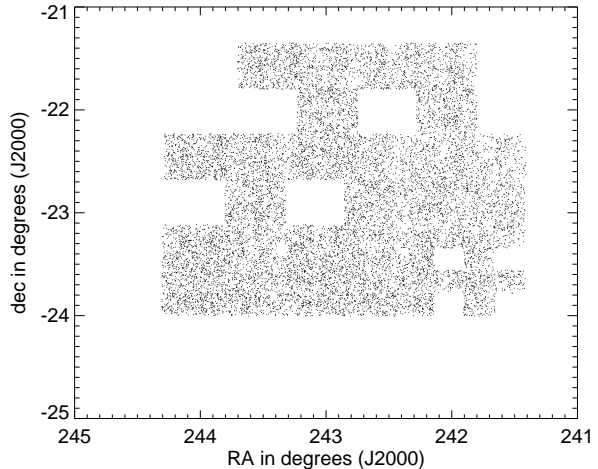


**Figure 1.** Tile coverage from the UKIDSS GCS Science Verification in the Upper Sco association. The total area covered is 6.5 square degrees. Note the somewhat uneven tile coverage from the GCS science verification phase.

$Y = 19.8$ ,  $J = 18.7$ ,  $H = 18.1$ ,  $K = 17.3$  mag in the case of the science verification data in Upper Sco (Fig. 2). We should mention that WFCAM was not quite in its final best focus mode so that those completeness limits will be improved for the upcoming releases. We refer the reader to Lawrence et al. (2006) for more details on the observing strategy of the UKIDSS project.

All observations carried out by the UKIDSS project<sup>1</sup> are pipeline-processed at the Cambridge Astronomical Survey Unit (CASU; Irwin et al. 2006, in preparation)<sup>2</sup>. The processed data are then archived in Edinburgh and released to the user community through the WFCAM Science Archive (WSA; Hambly et al. 2006, in preparation)<sup>3</sup>.

We have selected all point sources ( $yjkhClass = -1$  or  $-2$ ) in the Upper Sco association taken during the Science Verification phase. The Class parameter refers to a morphological classification of a source in each passband where  $-1$  is a point source,  $-2$  is borderline stellar,  $0$  is noise, and  $+1$  is nonstellar (more details can be found in the online glossary within the WFCAM Science Archive pages). We have selected sources detected in all of *YJHK* with no requirement for detection in *Z* in order to increase our sensitivity to cooler objects. The query included the cross-correlation

<sup>1</sup> [www.ukidss.org](http://www.ukidss.org)

<sup>2</sup> The CASU WFCAM webpage can be found at <http://apm15.ast.cam.ac.uk/wfcam>

<sup>3</sup> The WFCAM Science Archive is accessible at <http://surveys.roe.ac.uk/wsa>

**Table 2.** Log of the observations. Central coordinates (in J2000) of each WFCAM tile is provided along with the observing date. Each tile was observed in all five passbands (*ZYJHK*).

Tile	R.A.	Dec.	Date
1	16 8	-22 40	2005-04-18
2	16 8	-23 33	2005-04-18
3	16 9	-21 48	2005-04-11
4	16 11	-22 41	2005-04-11
5	16 11	-23 33	2005-04-18
6	16 13	-21 48	2005-04-11
7	16 15	-22 41	2005-04-11
8	16 15	-23 33	2005-04-18

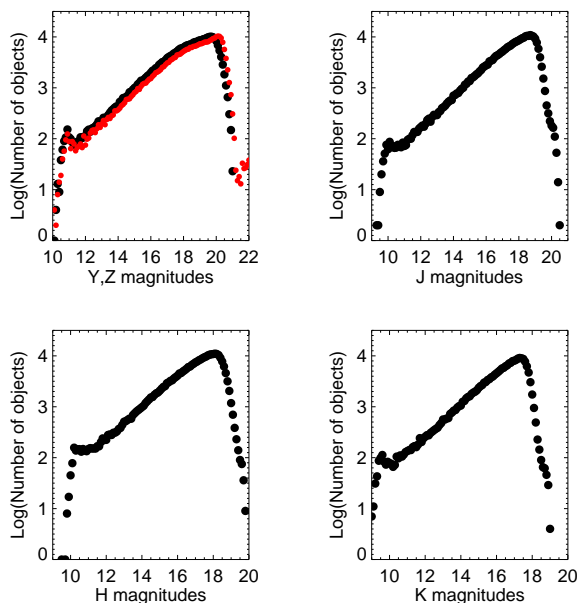


**Figure 2.** Number–magnitude histograms for Upper Sco observations in all filters, including *Z* and *Y* (top left), *J* (top right), *H* (bottom left), and *K* (bottom right). The 100% completeness limits are estimated to  $Z = 20.1$ ,  $Y = 19.8$ ,  $J = 18.7$ ,  $H = 18.1$ ,  $K = 17.3$ , respectively. The completeness limits are defined as the magnitude where the histogram stops following a straight line in a logarithmic scale.

with 2MASS to compute their proper motion thanks to a 5 year baseline between the GCS and 2MASS observations in Upper Sco. The query returned a total of 133,476 sources fainter than  $Z = 11.4$  and  $J = 10.5$  mag to avoid contamination from saturated stars. The magnitudes are AperMag3 magnitudes and the colours originate from the difference of those magnitudes. Those AperMag3 magnitudes represent the flux of a point source within an aperture with a diameter of 1 arcsec. The Structured Query Language query used to select the initial sample is given in Appendix A, along with an explanation. The coverage, displayed in Fig. 1, is about 6.5 square degrees. The resulting colour–magnitude diagram is shown in Fig. 3 and is analysed in the next section.

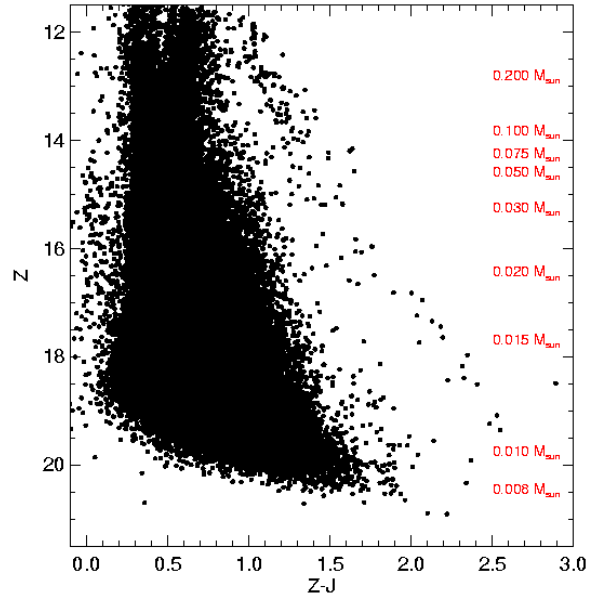


**Figure 3.** ( $Z - J, Z$ ) colour–magnitude diagram for a 6.5 square degree area covered in the Upper Sco association within the science verification phase of the UKIDSS Galactic Cluster Survey. The gap between the members of the association and field stars is clearly demarcated. The mass scale is shown on the right hand side of the diagrams and extends below  $0.01 M_{\odot}$ , according to the DUSTY models.

### 3 NEW ASSOCIATION MEMBERS IN UPPER SCO

This section describes the selection of cluster candidates in Upper Sco based on various colour–magnitude diagrams drawn from the *ZYJHK* broadband filters and proper motion using 2MASS (Cutri et al. 2003) as a measure of first epoch positions for the brighter objects.

#### 3.1 Colour–magnitude diagrams

The depth and coverage of the GCS observations provides *ZYJHK* photometry of 133,476 point sources in Upper Sco over 6.5 square degrees with  $Z = 11.4$ – $21.5$  mag. We have plotted in Fig. 5 four colour–magnitude diagrams to select potential cluster candidates and assess their membership. On the top panels in Fig. 5 we show the ( $Z - J, Z$ ) and ( $Z - K, Z$ ) diagrams whereas the ( $Y - J, Y$ ) and ( $J - K, J$ ) diagrams are displayed in the lower panels. Overplotted are 5 and 10 Myr NextGen (solid lines; Baraffe et al. 1998), DUSTY (dashed lines; Chabrier et al. 2000), and COND (dotted lines; Baraffe et al. 2002) isochrones shifted at the distance of the association ( $d = 145$  pc).

#### 3.2 Selection of cluster candidates

The extraction of candidates in open clusters usually consists in selecting sources to the right of the Zero Age Main Sequence (Leggett 1992) or theoretical isochrones (Baraffe et al. 1998) shifted to the distance of the cluster. This method has been applied at optical and near–infrared wavelengths in numerous

**Table 3.** Summary of quality indicators for the observations, averaged over all detector frames of a given filter. These illustrate the quality of the science verification data, and are not typical of the UKIDSS surveys in general (Dye et al. 2006). Magnitudes are on the Vega magnitude scale in the natural WFCAM Mauna Kea Observatories (MKO) photometric system, as defined in Hewett et al. (2006) and references therein.

Filter	Seeing / arcsec			Average stellar ellipticity			Photometric zeropoint			5 $\sigma$ detection limit		
	min	mean	max	min	mean	max	min	mean	max	min	mean	max
Z	0.80	1.02	1.41	0.036	0.111	0.239	22.68	22.72	22.76	19.91	20.31	20.79
Y	0.84	1.04	1.38	0.040	0.105	0.241	22.64	22.67	22.69	19.45	19.86	20.17
J	0.70	0.90	1.24	0.031	0.110	0.273	24.40	24.48	24.49	19.17	19.41	19.67
H	0.68	0.86	1.02	0.030	0.098	0.238	24.68	24.72	24.73	18.49	18.77	19.03
K	0.77	0.95	1.18	0.036	0.123	0.274	24.01	24.03	24.04	17.74	18.02	18.18

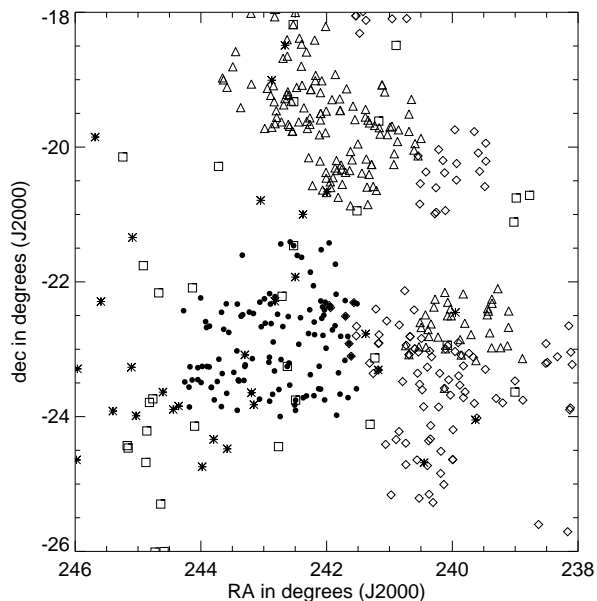


**Figure 4.** Comparison between previous and the current surveys conducted in the Upper Sco association. New candidates from our study are shown as filled circles. We have included known members from Preibisch & Zinnecker (2002) (triangles), Ardila et al. (2000) (diamonds), Martín et al. (2004) (squares), and Slesnick et al. (2006) (star symbols). Four sources are common to our study and those of Martín et al. (2004) and Slesnick et al. (2006).

clusters, including the Pleiades (Zapatero Osorio et al. 1997),  $\alpha$  Per (Barrado y Navascués et al. 2002), IC 2391 (Barrado y Navascués et al. 2001), and others. The contamination by field stars along the line of sight is estimated to about 20–40% across the hydrogen burning limit (Moraux et al. 2001; Barrado y Navascués et al. 2002).

The sequence of members in Upper Sco is well separated from field stars in the  $(Z - J, Z)$  colour–magnitude diagram and matches well the theoretical isochrones over the 0.3–0.008  $M_{\odot}$  mass range ( $Z = 11.5$ – $20.5$  mag). The masses indicated to the right hand side of each diagram come from the NextGen models for objects more massive than 0.05  $M_{\odot}$  and DUSTY isochrones for lower masses, assuming an age of 5 Myr and a distance of 145 pc for the association (Preibisch & Zinnecker 2002).

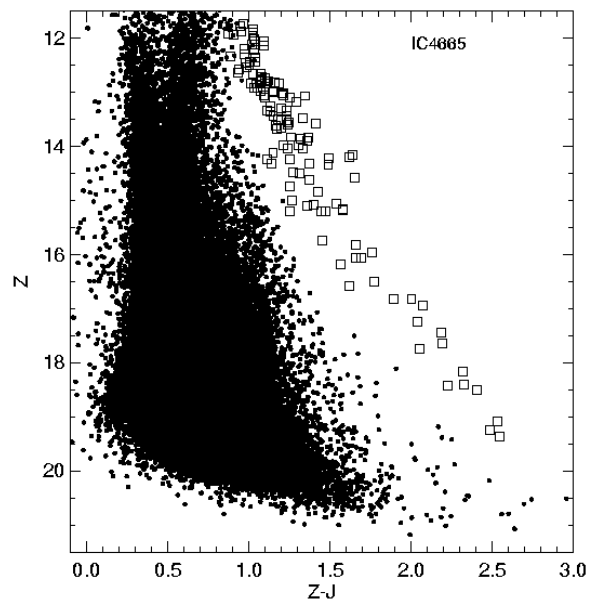


**Figure 7.**  $(Z - J, Z)$  colour–magnitude diagram for a 2.4 square degree area covered in the IC4665 open cluster during the science verification phase of the UKIDSS Galactic Cluster Survey. We have superimposed the sequence of Upper Sco members (open squares) to illustrate the low contamination of our sample.

We have selected a total of 164 sources to the right of three segments defined by:

- $(Z - J, Z) = (0.8, 11.5)$  and  $(1.4, 17.0)$
- $(Z - J, Z) = (1.4, 17.0)$  and  $(2.1, 19.5)$
- All objects satisfying  $Z - J > 2.1$  and  $J < 19.5$  mag

We believe that our selection is conservative as we included all cluster members and field stars lying on the blue side of the gap between the association and field sequences. This selection also allows for the line-of-sight depth of the association. Field dwarfs and background stars contaminating our sample are excluded from the original list after investigation of their location in other colour–magnitude diagrams and in the proper motion vector point diagram (see later). For example, we found 18 sources (open squares) lying clearly either on the blue side or the red side of the association sequence in the other colour–magnitude diagrams displayed in Fig. 5 and in the  $(Z - K, J - K)$  colour–colour diagram (Fig. 6). Consequently, 146 candidates remain probable photo-

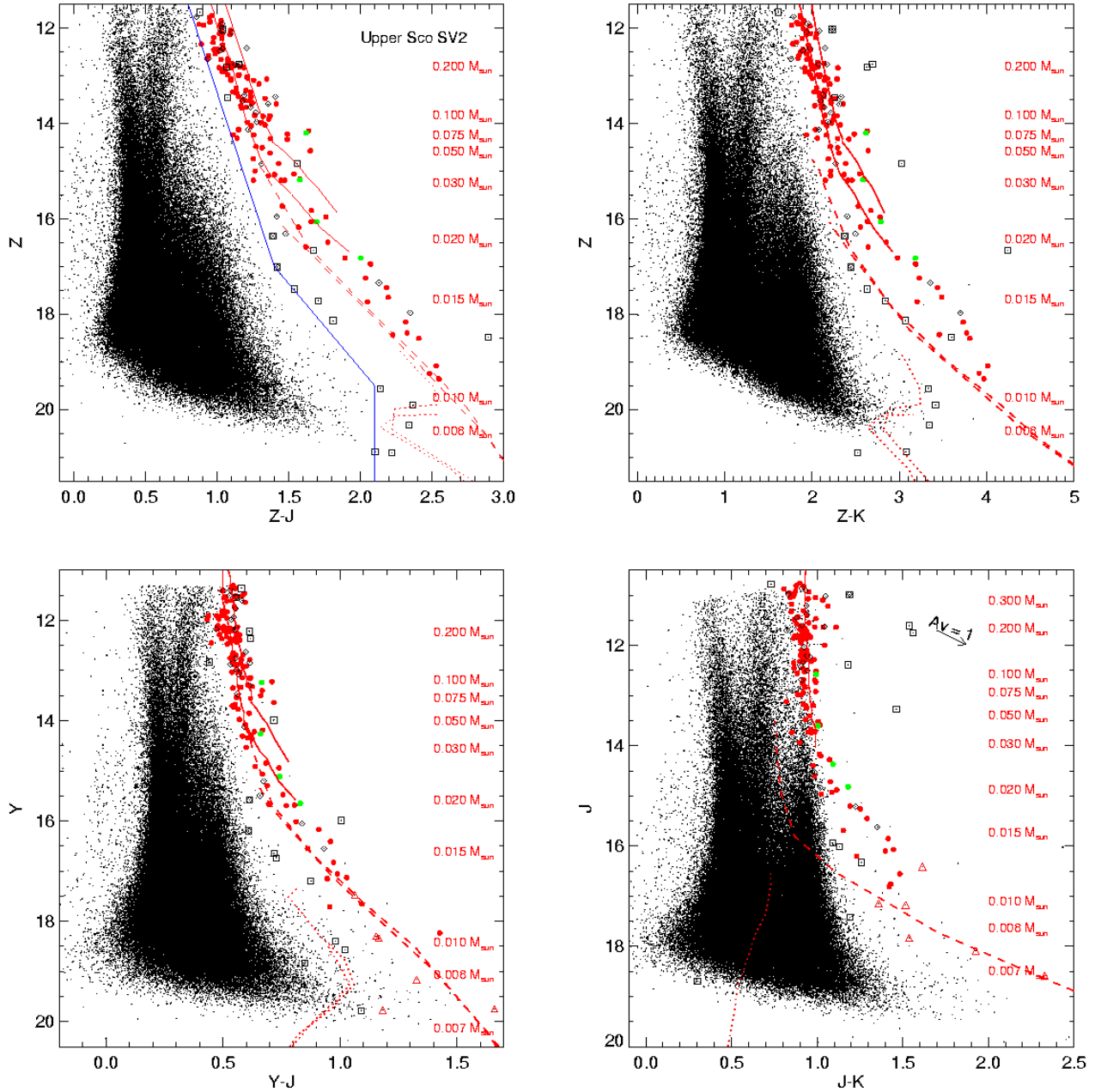


**Figure 5.** Colour-magnitude diagrams for 6.5 square degrees in Upper Sco from the UKIDSS Galactic Cluster Survey. Red circles represent the selected candidates in Upper Sco from the GCS Science Verification. Open triangles are new faint candidates with no  $Z$ -band detection extracted from the  $(Y - J, Y)$  colour-magnitude diagram. Photometric non-members and proper motion non-members are displayed as open squares and open diamonds, respectively. Green circles are spectroscopic members recovered in our study (Martín et al. 2004; Slesnick et al. 2006). Overplotted are the 5 and 10 Myr NextGen (solid line; Baraffe et al. 1998), DUSTY (dashed line; Chabrier et al. 2000), and COND (dotted line; Baraffe et al. 2002) isochrones. The mass scale is shown on the right hand side of the diagrams and spans 0.3–0.01  $M_{\odot}$ , according to the NextGen and DUSTY models. *Top left:*  $(Z - J, Z)$  diagram. *Top right:*  $(Z - K, Z)$  diagram. *Bottom left:*  $(Y - J, Y)$  diagram. *Bottom right:*  $(J - K, J)$  diagram. Note that the theoretical isochrones were specifically computed for the WFCAM set of filters (courtesy I. Baraffe and F. Allard).

metric members. We further investigate their membership in Sect. 3.3 using their proper motion. We note that our study recovered 4 spectroscopic members (Table 5; green filled circles in Figs. 5 & 6) unveiled by Martín et al. (2004) and Slesnick et al. (2006). One of them, DENIS J160958–234519

was reported as binary member of Upper Sco by Bouy et al. (2006).

We would like to emphasize that the contamination of our sample by field dwarfs or background stars is negligible. To corroborate this statement, we have extracted from the WSA all point sources towards the young open clus-

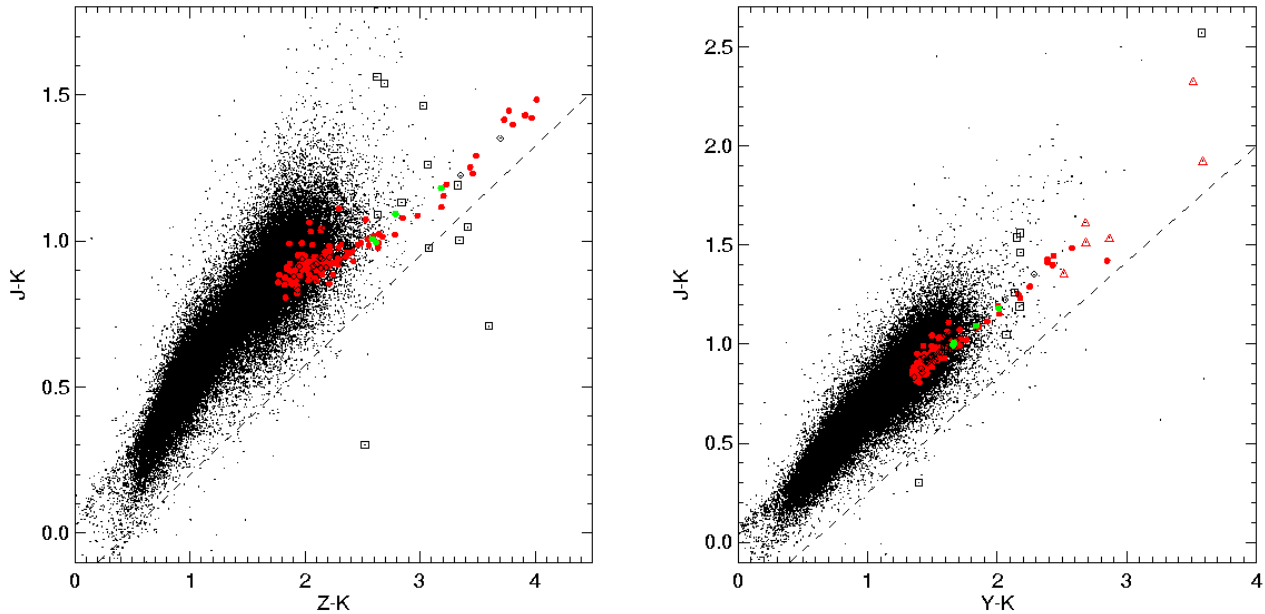


**Figure 6.**  $(Z - K, J - K)$  and  $(Y - K, J - K)$  two-colour diagrams for 6.5 square degrees in Upper Sco from the UKIDSS Galactic Cluster Survey. Red circles represent the new candidates in Upper Sco and open triangles new faint candidates with no  $Z$ -band detection. Open squares and open diamonds are photometric and proper motion non-members, respectively. Green circles are spectroscopic members (Martín et al. 2004; Slesnick et al. 2006) recovered in our study.

ter IC4665 (50–100 Myr; 350 pc) and found 2 contaminants after applying the same photometric and proper motion selection. This result represent an upper limit on the contamination as IC4665 is at lower galactic latitude than Upper Sco ( $b \sim 10^\circ$  vs.  $20^\circ$ ), while the surveyed area is similar. Figure 7 shows the  $(Z - J, Z)$  colour-magnitude diagram for IC4665 with the Upper Sco members superimposed (open squares). It is immediately obvious from this diagram that the field contamination must be very low.

Furthermore, we have searched for lower mass brown dwarfs by selecting faint candidates in the  $(Y - J, Y)$  colour-magnitude diagram with no  $Z$ -band detections, yielding 15 new candidates (red open triangles in Figs. 5 & 6). The  $(J - K, J)$  diagram suggests however that several of them are likely contaminants since their  $J - K$  colours are too blue. This leaves 6 sources worthy of spectroscopic follow-up after retaining sources redder than  $J - K = 1.2$ . One object (USco J160843.4–224516;  $J = 18.6$ ;  $J - K = 2.3$ ) would be the faintest and coolest brown dwarf found in Upper Sco if confirmed as a member. Its mass and effective temperature would be estimated as  $\sim 7 M_{\text{Jup}}$  and  $\sim 1700$  K by the DUSTY models (Chabrier et al. 2000). The mass estimate should be interpreted with caution as Mohanty et al. (2004) derived masses from high-resolution spectroscopy discrepant by a factor of 2 with model predictions for the two faintest brown dwarfs found in Upper Sco prior to our survey. Our survey reaches three magnitudes deeper than any previous study in the region and has uncovered a large number of new low-mass brown dwarfs below  $0.02 M_{\odot}$ .

### 3.3 Proper motions

To further assess the membership of the brightest ( $J \leq 15.8$ ) candidates, we have cross-correlated the 2MASS database with the GCS observations to extract proper motions. The standard pipeline astrometric reductions of WFCAM data (Irwin et al. 2006, in preparation) use the 2MASS point source catalogue to provide secondary astrometric standards. Hence, on scale lengths of the order of the WFCAM detector size ( $\sim 10$  arcmin) all positional systematic errors are mapped out with respect to 2MASS and a straightforward difference between WFCAM and 2MASS epoch positions, divided by the epoch difference, yields *relative* proper motions. Proper motions derived using such a method are relative in the sense that the majority of stars in each field are moving slowly enough to be assumed to be stationary, and therefore define a zeropoint reference frame with respect to which peculiar cluster motions can be measured. Note, however, that such proper motions are in no sense absolute and are not on the inertial system defined by *Hipparcos*, regardless of the absolute positions being ultimately tied to the International Coordinate Reference System via the Tycho-2 catalogue reductions applied to 2MASS. Nonetheless, within the errors to which the proper motions are determined, they are comparable to absolute proper motions of high mass cluster members determined by *Hipparcos* since the underlying assumption of approximately zero net background stellar proper motions in these fields is valid.

The resulting vector point diagram (proper motion in right ascension versus proper motion in declination) for candidates brighter than  $J = 15.8$  mag (corresponding to  $15 M_{\text{Jup}}$  according to the DUSTY models) is shown in Fig. 8. In order to assess the likely errors in the proper motions so de-

**Table 4.** Near-infrared (*ZYJHK*) photometry for 129 member candidates in Upper Sco selected on the basis of their infrared colours. This table lists the equatorial coordinates (at equinox J2000), the magnitudes from the GCS and their associated errors taken from the WSA archive, as well as their proper motions. Proper motions are set arbitrarily to 99.9 when unavailable (13 objects); 116 objects have proper motions consistent with cluster membership.

R.A.	Dec.	Z	Y	J	H	K	$\mu_{\alpha} \cos \delta$	$\mu_{\delta}$
16 06 03.75	-22 19 30.0	18.169±0.036	16.825±0.014	15.853±0.009	15.096±0.009	14.438±0.009	13.7	-26.5
16 06 06.29	-23 35 13.3	18.430±0.041	17.150±0.018	16.204±0.012	15.540±0.012	14.973±0.012	99.9	99.9
16 06 15.95	-22 18 28.0	14.307±0.003	13.705±0.002	13.166±0.002	12.570±0.001	12.248±0.002	-5.0	-15.2
16 06 26.37	-23 06 11.4	14.477±0.003	13.770±0.002	13.205±0.002	12.616±0.001	12.271±0.002	0.7	-22.0
16 06 34.61	-22 55 04.4	13.049±0.002	12.366±0.001	11.835±0.001	11.243±0.001	10.873±0.001	-13.4	-8.8
16 06 38.24	-23 43 03.8	11.867±0.001	11.413±0.001	10.915±0.001	10.438±0.000	10.041±0.000	-13.5	-25.6
16 06 39.22	-22 48 34.2	13.520±0.002	12.874±0.001	12.322±0.001	11.742±0.001	11.422±0.001	-9.5	-19.6
16 06 48.18	-22 30 40.1	16.818±0.013	15.697±0.007	14.926±0.005	14.353±0.005	13.839±0.006	-22.7	-14.8
16 06 49.10	-22 16 38.4	15.094±0.004	14.339±0.003	13.735±0.002	13.199±0.002	12.881±0.003	-6.8	-26.5
16 06 50.18	-23 09 54.0	12.971±0.001	12.388±0.001	11.816±0.001	11.241±0.001	10.902±0.001	-22.9	-10.9
16 07 06.33	-22 48 28.2	12.644±0.001	12.129±0.001	11.567±0.001	10.967±0.001	10.686±0.001	-11.4	-21.6
16 07 08.81	-23 39 59.9	12.653±0.001	12.127±0.001	11.624±0.001	11.044±0.000	10.714±0.001	-4.7	-14.5
16 07 14.79	-23 21 01.2	19.085±0.076	17.649±0.029	16.556±0.017	16.556±0.017	15.072±0.015	99.9	99.9
16 07 21.96	-23 58 45.3	14.241±0.003	13.543±0.002	12.985±0.001	12.422±0.001	12.077±0.001	-8.3	-18.7
16 07 23.82	-22 11 02.0	17.239±0.016	16.015±0.009	15.202±0.006	14.564±0.004	14.009±0.005	-11.0	-30.7
16 07 26.41	-21 44 17.1	16.171±0.008	15.289±0.006	14.601±0.004	14.059±0.003	13.615±0.004	-13.2	-31.4
16 07 27.82	-22 39 04.0	19.358±0.100	18.236±0.048	16.810±0.022	16.091±0.023	15.388±0.023	99.9	99.9
16 07 37.99	-22 42 47.0	19.240±0.090	17.713±0.029	16.757±0.019	16.001±0.020	15.327±0.020	99.9	99.9
16 07 45.21	-22 22 57.6	13.589±0.002	12.935±0.001	12.348±0.001	11.811±0.001	11.485±0.001	-17.4	-21.1
16 07 50.39	-22 21 02.2	13.509±0.002	12.852±0.001	12.277±0.001	11.713±0.001	11.295±0.001	-13.9	-10.6
16 07 50.49	-21 25 20.2	14.029±0.003	13.319±0.002	12.693±0.001	12.100±0.001	11.707±0.001	-13.9	-16.8
16 08 02.17	-22 59 05.9	13.470±0.002	12.691±0.001	12.135±0.001	11.548±0.001	11.211±0.001	-8.8	-14.9
16 08 05.54	-22 18 07.1	11.728±0.001	11.306±0.001	10.762±0.000	10.244±0.000	9.862±0.000	-20.0	-17.3
16 08 07.45	-23 45 05.6	16.056±0.008	15.067±0.005	14.398±0.003	13.864±0.003	13.422±0.004	-7.7	-11.8
16 08 08.47	-22 25 00.1	12.572±0.001	12.109±0.001	11.631±0.001	10.998±0.000	10.726±0.001	-5.0	-22.5
16 08 10.81	-22 29 42.9	13.903±0.002	13.156±0.002	12.542±0.001	12.030±0.001	11.659±0.001	-5.9	-12.1
16 08 14.00	-22 47 39.4	12.808±0.001	12.173±0.001	11.649±0.001	11.029±0.001	10.735±0.001	-4.9	-15.0
16 08 15.66	-22 22 20.1	11.773±0.001	11.360±0.001	10.825±0.000	10.241±0.000	9.903±0.000	-8.6	-27.4
16 08 18.43	-22 32 25.0	18.507±0.042	17.128±0.016	16.099±0.010	15.438±0.011	14.700±0.010	99.9	99.9
16 08 20.79	-21 31 23.6	12.792±0.002	12.212±0.001	11.677±0.001	11.080±0.000	10.777±0.001	-7.8	-15.5
16 08 22.29	-22 17 03.0	14.312±0.003	13.557±0.002	12.939±0.001	12.394±0.001	12.020±0.001	-13.1	-11.0
16 08 23.03	-23 35 29.5	11.901±0.001	11.467±0.001	10.875±0.001	10.562±0.000	10.069±0.000	-11.4	-21.1
16 08 28.47	-23 15 10.4	17.643±0.020	16.408±0.010	15.449±0.007	14.776±0.006	14.157±0.006	-11.6	-12.6
16 08 30.49	-23 35 11.0	16.949±0.014	15.685±0.007	14.879±0.005	14.290±0.004	13.763±0.005	-4.5	-12.2
16 08 43.44	-22 45 16.0	99.999±9.999	19.768±0.178	18.585±0.097	17.224±0.062	16.257±0.051	99.9	99.9
16 08 46.06	-22 46 59.4	12.844±0.001	12.279±0.001	11.794±0.001	11.132±0.001	10.844±0.001	-12.5	-11.1
16 08 47.44	-22 35 47.9	17.738±0.022	16.550±0.011	15.688±0.007	15.086±0.008	14.534±0.009	0.3	-19.8
16 08 48.37	-23 41 21.0	13.833±0.002	13.036±0.002	12.463±0.001	11.907±0.001	11.545±0.001	-5.0	-20.2
16 08 50.34	-22 03 28.7	12.786±0.002	12.214±0.001	11.709±0.001	11.095±0.000	10.778±0.001	-11.1	-29.2
16 09 01.98	-21 51 22.7	15.165±0.005	14.221±0.003	13.587±0.002	13.035±0.001	12.570±0.002	1.0	-21.9
16 09 02.01	-23 22 40.3	12.006±0.001	11.530±0.001	10.973±0.001	10.475±0.000	10.106±0.000	-2.5	-36.1
16 09 04.51	-22 24 52.5	14.568±0.003	13.636±0.002	12.918±0.001	12.374±0.001	11.926±0.001	-11.9	-10.1
16 09 09.39	-22 45 59.1	12.441±0.001	11.895±0.001	11.398±0.001	10.787±0.000	10.457±0.001	-25.8	-12.2
16 09 16.89	-23 41 32.6	13.169±0.002	12.433±0.001	11.876±0.001	11.286±0.001	10.963±0.001	-18.9	-12.7
16 09 18.69	-22 29 23.7	99.999±9.999	19.744±0.143	18.083±0.055	17.061±0.047	16.157±0.039	99.9	99.9
16 09 29.39	-23 43 12.2	15.961±0.007	14.941±0.004	14.202±0.003	13.640±0.003	13.180±0.003	-0.8	-19.7
16 09 35.75	-21 38 05.8	11.835±0.001	11.360±0.001	10.807±0.000	10.337±0.000	9.930±0.000	2.4	-18.7
16 09 39.68	-22 31 53.9	12.708±0.001	12.163±0.001	11.630±0.001	11.001±0.000	10.644±0.001	-12.4	-23.6
16 09 46.33	-22 55 33.6	13.096±0.002	12.448±0.001	11.998±0.001	11.286±0.001	10.953±0.001	-18.5	-18.9
16 09 52.17	-21 36 27.8	14.154±0.003	13.224±0.002	12.515±0.001	11.966±0.001	11.521±0.001	-10.4	-14.3
16 09 56.34	-22 22 45.5	99.999±9.999	19.158±0.126	17.830±0.060	16.993±0.038	16.293±0.043	99.9	99.9
16 09 58.52	-23 45 18.7	14.195±0.003	13.238±0.002	12.574±0.001	12.034±0.001	11.578±0.001	-14.0	-21.8
16 09 58.78	-23 54 27.5	12.494±0.001	11.972±0.001	11.490±0.001	10.944±0.000	10.624±0.001	-24.6	-24.9
16 10 01.84	-23 49 43.4	12.045±0.001	11.504±0.001	10.949±0.001	10.498±0.000	10.111±0.000	-10.6	-20.7
16 10 06.08	-21 27 44.1	16.823±0.013	15.650±0.007	14.820±0.004	14.219±0.003	13.638±0.004	-0.6	-17.1
16 10 19.03	-21 24 25.2	12.784±0.002	12.204±0.001	11.665±0.001	11.100±0.000	10.735±0.001	-12.5	-18.8
16 10 20.87	-23 31 55.7	13.015±0.002	12.355±0.001	11.801±0.001	11.267±0.001	10.930±0.001	-12.8	-8.9
16 10 23.44	-23 12 17.7	12.133±0.001	11.636±0.001	11.041±0.001	10.678±0.000	10.197±0.000	-0.9	-15.5
16 10 26.50	-22 30 53.4	12.446±0.001	11.904±0.001	11.467±0.001	10.973±0.000	10.475±0.001	5.7	-17.7
16 10 30.14	-23 15 16.8	16.062±0.008	15.110±0.005	14.367±0.003	13.786±0.003	13.275±0.003	-1.9	-16.8
16 10 47.13	-22 39 49.4	17.442±0.020	16.167±0.011	15.258±0.007	14.567±0.005	14.006±0.006	-15.1	-23.6
16 10 54.29	-23 09 11.1	14.125±0.003	13.531±0.002	12.975±0.001	12.440±0.001	12.090±0.001	-15.1	-32.6



R.A.	Dec.	$Z$	$Y$	$J$	$H$	$K$	$\mu_{\alpha} \cos \delta$	$\mu_{\delta}$
16 10 54.99	-21 26 14.0	14.222±0.003	13.398±0.002	12.730±0.001	12.156±0.001	11.738±0.001	-7.8	-16.8
16 10 57.28	-23 59 54.1	14.044±0.003	13.346±0.002	12.803±0.001	12.212±0.001	11.877±0.001	-8.9	-19.8
16 11 02.11	-23 35 50.6	13.024±0.002	12.371±0.001	11.817±0.001	11.225±0.001	10.872±0.001	-27.9	-31.2
16 11 07.38	-22 28 50.3	13.585±0.002	12.785±0.002	12.171±0.001	11.641±0.001	11.226±0.001	0.0	-28.9
16 11 17.05	-22 13 08.8	12.826±0.002	12.154±0.001	11.639±0.001	10.982±0.000	10.528±0.001	-19.2	-26.1
16 11 19.07	-23 19 20.4	12.736±0.001	12.171±0.001	11.635±0.001	10.951±0.000	10.598±0.001	-15.0	-18.2
16 11 23.99	-22 53 32.6	12.537±0.001	11.981±0.001	11.549±0.001	10.937±0.000	10.599±0.001	-11.0	-7.2
16 11 26.30	-23 40 06.1	14.834±0.004	13.975±0.003	13.404±0.002	12.822±0.001	12.448±0.002	-1.2	-24.8
16 11 31.81	-22 37 08.3	13.984±0.003	13.286±0.002	12.679±0.001	12.115±0.001	11.758±0.001	-1.7	-16.6
16 11 34.70	-22 19 44.3	14.613±0.004	13.854±0.003	13.242±0.002	12.693±0.001	12.304±0.001	-4.3	-14.7
16 11 37.61	-23 46 14.8	13.302±0.002	12.643±0.001	12.099±0.001	11.478±0.001	11.158±0.001	-21.5	-9.6
16 11 37.84	-22 10 27.5	12.107±0.001	11.606±0.001	11.069±0.001	10.543±0.000	10.122±0.000	-4.2	-26.1
16 11 38.37	-23 07 07.5	15.190±0.004	14.367±0.003	13.743±0.002	13.204±0.002	12.777±0.002	-12.1	-31.9
16 11 40.40	-23 11 34.9	13.847±0.002	13.143±0.002	12.525±0.001	11.987±0.001	11.600±0.001	-4.7	-15.5
16 11 54.39	-22 36 49.3	15.730±0.007	14.912±0.005	14.274±0.003	13.628±0.002	13.201±0.003	0.4	-11.9
16 11 57.37	-22 15 06.8	15.071±0.004	14.287±0.003	13.668±0.002	13.095±0.001	12.705±0.002	-13.1	-15.9
16 12 09.48	-22 39 57.1	12.189±0.001	11.764±0.001	11.212±0.001	10.425±0.000	10.149±0.000	-7.8	-8.9
16 12 14.92	-22 18 04.0	13.500±0.002	12.882±0.002	12.320±0.001	11.726±0.001	11.398±0.001	-3.6	-16.5
16 12 16.09	-23 44 25.0	14.505±0.003	13.737±0.002	13.188±0.002	12.545±0.001	12.212±0.002	-7.3	-18.9
16 12 27.64	-21 56 40.8	99.999±9.999	18.296±0.050	17.141±0.028	16.371±0.020	15.782±0.024	99.9	99.9
16 12 28.95	-21 59 36.1	99.999±9.999	17.471±0.025	16.407±0.015	15.565±0.010	14.791±0.010	99.9	99.9
16 12 39.54	-22 28 08.3	12.348±0.001	11.826±0.001	11.308±0.001	10.714±0.000	10.389±0.001	-20.1	-16.6
16 12 43.74	-23 08 23.2	12.986±0.002	12.393±0.001	11.836±0.001	11.244±0.001	10.892±0.001	-17.5	-11.0
16 12 46.92	-23 38 40.9	15.180±0.005	14.261±0.003	13.601±0.002	13.022±0.002	12.595±0.002	-5.3	-17.1
16 12 55.28	-22 26 54.4	13.564±0.002	12.913±0.002	12.314±0.001	11.710±0.001	11.347±0.001	-6.7	-27.6
16 13 02.32	-21 24 28.4	99.999±9.999	18.335±0.049	17.169±0.023	16.371±0.019	15.652±0.022	99.9	99.9
16 13 10.82	-23 13 51.6	13.621±0.002	13.018±0.002	12.454±0.001	11.940±0.001	11.590±0.001	-7.2	-40.8
16 13 12.16	-23 15 16.6	12.782±0.001	12.261±0.001	11.702±0.001	11.104±0.001	10.791±0.001	-4.3	-25.3
16 13 15.65	-23 27 44.2	11.918±0.001	11.548±0.001	11.043±0.001	10.279±0.000	10.053±0.000	-7.4	-8.7
16 13 20.53	-22 29 16.0	11.929±0.001	11.531±0.001	11.021±0.001	10.578±0.000	10.162±0.000	-17.2	-11.1
16 13 21.91	-21 36 13.7	11.955±0.001	11.513±0.001	10.930±0.000	10.359±0.000	9.978±0.000	-6.8	-18.9
16 13 26.66	-22 30 35.0	15.053±0.004	14.185±0.003	13.515±0.002	12.959±0.001	12.509±0.002	5.6	-20.8
16 13 34.76	-23 28 15.7	14.738±0.004	14.081±0.003	13.485±0.002	12.914±0.002	12.553±0.002	-6.0	-16.8
16 13 36.47	-23 27 35.5	13.332±0.002	12.683±0.001	12.098±0.001	11.545±0.001	11.189±0.001	-13.5	-23.1
16 13 36.88	-23 27 29.9	12.828±0.001	12.327±0.001	11.812±0.001	11.191±0.001	10.912±0.001	-16.7	-16.7
16 13 40.79	-22 19 46.1	16.494±0.010	15.477±0.007	14.721±0.004	14.153±0.003	13.643±0.004	-14.4	-18.1
16 13 41.30	-23 54 22.0	13.048±0.002	12.470±0.001	11.951±0.001	11.377±0.001	11.043±0.001	-26.4	-24.2
16 13 42.64	-23 01 28.0	15.189±0.005	14.337±0.003	13.718±0.002	13.149±0.002	12.730±0.002	-13.1	-13.8
16 13 54.34	-23 20 34.4	12.114±0.001	11.611±0.001	11.095±0.001	10.493±0.000	10.063±0.000	-8.0	-24.7
16 14 13.52	-22 44 58.0	13.434±0.002	12.825±0.002	12.283±0.001	11.680±0.001	11.344±0.001	-7.0	-20.7
16 14 21.44	-23 39 14.8	16.587±0.010	15.663±0.006	14.968±0.005	14.445±0.005	13.944±0.006	0.2	-18.0
16 14 23.12	-22 19 33.9	13.064±0.002	12.288±0.001	11.717±0.001	11.186±0.001	10.785±0.001	-10.1	-11.2
16 14 32.87	-22 42 13.5	15.823±0.007	14.846±0.005	14.163±0.003	13.633±0.002	13.149±0.003	-10.6	-18.9
16 14 38.46	-23 21 37.3	12.327±0.001	11.909±0.001	11.436±0.001	10.860±0.000	10.551±0.001	-16.0	-16.0
16 14 41.19	-22 27 05.4	12.745±0.001	12.149±0.001	11.664±0.001	11.021±0.000	10.757±0.001	-13.5	-27.5
16 14 41.68	-23 51 05.9	18.395±0.040	17.059±0.017	16.069±0.010	15.337±0.010	14.623±0.010	99.9	99.9
16 14 51.31	-23 08 51.7	13.670±0.002	13.036±0.002	12.497±0.001	11.895±0.001	11.565±0.001	-8.5	-22.2
16 14 57.50	-23 28 42.8	12.626±0.001	12.173±0.001	11.695±0.001	11.073±0.001	10.787±0.001	-18.1	-12.6
16 15 08.92	-23 45 04.9	13.360±0.002	12.755±0.001	12.224±0.001	11.620±0.001	11.280±0.001	-9.9	-16.4
16 15 20.10	-23 33 54.7	14.329±0.003	13.500±0.002	12.838±0.001	12.344±0.001	11.907±0.001	7.6	-29.7
16 15 20.24	-23 33 59.0	12.910±0.002	12.367±0.001	11.873±0.001	11.266±0.001	10.955±0.001	-25.2	-16.9
16 15 27.43	-22 39 27.7	12.294±0.001	11.818±0.001	11.321±0.001	10.764±0.000	10.472±0.001	-14.1	-28.2
16 15 28.19	-23 15 44.1	14.236±0.003	13.675±0.002	13.123±0.001	12.634±0.001	12.302±0.002	-12.8	-23.8
16 15 36.48	-23 15 17.6	15.190±0.005	14.533±0.003	13.935±0.002	13.396±0.002	13.037±0.003	-1.6	-15.7
16 15 38.66	-22 40 37.3	13.826±0.002	13.144±0.002	12.562±0.001	12.022±0.001	11.677±0.001	-12.2	-31.8
16 15 42.06	-22 35 24.0	12.440±0.001	11.952±0.001	11.436±0.001	10.842±0.000	10.546±0.001	5.5	-20.8
16 15 54.87	-23 15 14.8	12.214±0.001	11.728±0.001	11.180±0.001	10.645±0.000	10.328±0.001	-21.0	-27.0
16 15 59.26	-23 29 36.5	13.333±0.002	12.765±0.001	12.221±0.001	11.631±0.001	11.309±0.001	-12.8	-17.8
16 16 00.81	-22 14 19.4	13.089±0.002	12.399±0.001	11.834±0.001	11.289±0.001	10.943±0.001	1.2	-12.8
16 16 11.72	-23 27 05.2	12.973±0.002	12.430±0.001	11.898±0.001	11.294±0.001	10.996±0.001	-15.8	-14.6
16 16 11.83	-23 16 26.9	13.971±0.002	13.335±0.002	12.758±0.001	12.180±0.001	11.843±0.001	-15.5	-11.0
16 16 33.43	-23 27 21.2	13.431±0.002	12.774±0.001	12.195±0.001	11.669±0.001	11.293±0.001	-13.1	-24.9
16 16 41.63	-23 15 39.1	12.911±0.001	12.395±0.001	11.854±0.001	11.287±0.001	10.992±0.001	-19.6	-15.6
16 16 43.96	-23 51 25.9	12.830±0.001	12.243±0.001	11.728±0.001	11.109±0.001	10.800±0.001	-3.6	-25.7
16 16 45.39	-23 33 41.6	14.992±0.004	14.310±0.003	13.726±0.002	13.180±0.002	12.779±0.002	-17.2	-30.3
16 17 01.47	-23 29 06.0	13.656±0.002	13.025±0.002	12.453±0.001	11.887±0.001	11.537±0.001	-17.9	-19.6
16 17 06.06	-22 25 41.6	13.254±0.002	12.663±0.002	12.120±0.001	11.516±0.001	11.202±0.001	-15.0	-26.4



**Table 5.** The four candidates with  $I$  magnitudes and spectral types already published recovered during our work. We list their coordinates (J2000),  $I$  magnitudes from Martín et al. (2004) and Slesnick et al. (2006),  $ZYJHK$  photometry from the GCS, proper motion, as well as  $H\alpha$  equivalent widths (Å) and spectral types taken from the literature. Note that DENIS-P J161030–231517 was rejected as a member by Martín et al. (2004) although we find its photometry and proper motion consistent with membership.

RA	dec	$I$	$Z$	$Y$	$J$	$H$	$K$	$\mu_\alpha \cos \delta$	$\mu_\delta$	EW( $H\alpha$ )	SpT
16 12 46.92	−23 38 40.9	15.90	15.179	14.261	13.600	13.022	12.594	−5.3	−17.1	−14.7	M6.0
16 09 58.50	−23 45 18.6	15.04	14.195	13.238	12.573	12.034	11.578	−14.0	−21.8	−20.0	M6.5
16 10 30.10	−23 15 16.7	17.04	16.062	15.109	14.367	13.786	13.275	−2.0	−16.8	−12.0	M7.5
16 10 06.00	−21 27 44.6	18.11	16.822	15.649	14.819	14.219	13.638	−0.6	−17.1	−17.0	M8.5

ried, we examined histograms of the distribution of proper motions for all stars matched between the GCS Upper Sco observations and 2MASS. Under the assumption that these distributions are dominated by centroiding errors and not real stellar motions, we estimate that the proper motion errors are  $\sim 10 \text{ mas yr}^{-1}$  in either coordinate, and we plot a typical error bar in Fig. 8, in addition to a  $2\sigma$  error selection circle about the mean association proper motion of  $(-11, -25) \text{ mas/yr}$  (de Bruijne et al. 1997; Preibisch et al. 1998). Most photometric candidates lie within the selection region and those candidates have thus high probability of being members of Upper Sco. We have classified 23 photometric candidates as proper motion non-members (open diamonds in Fig. 8) because they lie outside the  $2\sigma$  selection circle. For comparison, we have also overplotted a sample of field stars brighter than  $J = 15.8 \text{ mag}$  for which proper motion is available from the GCS/2MASS cross-correlation. We have selected them in the region delineated by  $\text{ra}=242.0\text{--}242.5^\circ$  and declination between  $-23.0$  and  $-22.5^\circ$  (small dots in Fig. 8). Clearly, candidates can not be selected on their proper motion alone. However, proper motion does act as a useful extra criterion to the photometry.

To summarise, we have extracted a total of 129 member candidates in Upper Sco (red symbols in Fig. 8) from the GCS Science Verification data as follows. An initial sample of 164 candidates was selected from the  $Z$ ,  $Z\text{--}J$  colour-magnitude diagram; 18 of those were rejected on the basis of their position in other CMDs, leaving 146 sources. A further 23 sources were rejected as having proper motions inconsistent with cluster membership, leaving 123 candidates. Finally, we added on 6  $Z$  ‘drop outs’ from  $Y$ ,  $Y\text{--}J$  CMD selection, yielding a total of 129 candidates (but note that the faintest 13 have no proper motion measurement as they are beyond the sensitivity limit of 2MASS).

## 4 DISCUSSION

### 4.1 New low-mass brown dwarfs

The lowest mass brown dwarfs discovered in Upper Sco were reported by Martín et al. (2004) with spectral types of M9. The faintest of them, DENIS-P J161452–201713 has  $J = 15.33 \text{ mag}$ . Our survey is 100% complete, within the area surveyed, down to  $J = 18.7 \text{ mag}$  i.e. over 3 magnitudes deeper than the faintest objects currently known in the association. We detect a dozen new brown dwarf candidates with masses below  $0.02 M_\odot$  (filled circles and open triangles in Fig. 5), according to the DUSTY models (Chabrier et al. 2000). These new brown dwarfs are the

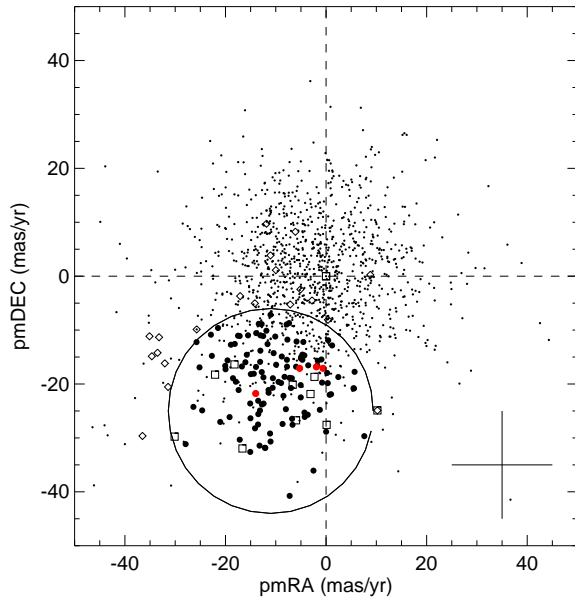


**Figure 8.** Vector point diagram (proper motion in right ascension versus proper motion in declination) for photometric candidate members in Upper Sco brighter than  $J = 15.8$  (filled circles). We have classified as non-members candidates lying outside a  $2\sigma$  circle centred on  $(-11, -25) \text{ mas/yr}$ , the mean proper motion of Upper Sco (de Bruijne et al. 1997; Preibisch et al. 1998). Photometric non-members and proper motion non-members are displayed as open squares and open diamonds, respectively. Small dots are field stars located in a  $0.25$  square region ( $\text{ra}=242.0\text{--}242.5^\circ$  and  $\text{dec}$  between  $-23.0$  and  $-22.5^\circ$ ) to illustrate the distribution of sources in this diagram when no photometric selection is applied. The four red filled circles represent spectroscopic members from Martín et al. (2004) and Slesnick et al. (2006). A typical proper motion error bar of  $10 \text{ mas/yr}$  is shown in the lower right hand side.

lowest mass substellar objects ever found in Upper Sco. However, Mohanty et al. (2004) derived lower masses than the model predictions for two M7–M8 dwarfs reported by Ardila et al. (2000) from higher resolution optical spectra, suggesting that we may be probing lower masses than these theoretical predictions indicate. Effective temperatures predicted by atmospheric models suggest that the lowest mass objects will be young L dwarfs. We plan to obtain optical and near-infrared spectroscopy to investigate the effect of gravity on the absorption bands and atomic features present in L dwarfs (McGovern et al. 2004).

We possibly detect the M7/M8 gap around  $0.03 M_\odot$

due to the formation of large dust grains at low temperature (Dobbie et al. 2002). This gap is consistent with the spectral types derived for the four members recovered by our study (green circles in Fig. 5; see also Sect. 4.2). Finally, there is a hint of a second gap below  $0.015 M_{\odot}$  which might represent the M/L transition. Statistics on those gaps will improve after full coverage of the association and we plan to investigate those effects in later papers exploiting the UKIDSS Galactic Clusters Survey.

## 4.2 Binaries

Our sample of candidates in Upper Sco includes four objects previously reported in the literature (green filled circles in Fig. 5). Three of them, DENIS-P J160958–234518, DENIS-P J161030–231516, and DENIS-P J161006–212744 were classified as M6.5, M7.5, and M7.5, respectively (Martín et al. 2004). The latter, however, was rejected as a member on the basis of the equivalent width of the NaI doublet ( $7.6\text{\AA}$ ). This object could be a field dwarf contaminant although it fits well the sequence of members in all colour–magnitude diagrams as well as in the proper motion vector point diagram. Radial velocity is required to further clarify the status of this object. The fourth object recovered, SCH161247–233841, was classified as a M6 member by Slesnick et al. (2006) who measured an  $H\alpha$  equivalent width of  $-14.7\text{\AA}$ .

We note that DENIS J160958–234518 lies clearly above the cluster sequence in the  $(Z - J, Z)$  colour–magnitude diagram and was announced as a close binary system at a separation of 0.08 arcsec by Bouy et al. (2006). Other red objects lying above the sequence in the  $(Z - J, Z)$  colour–magnitude diagram and redder in the  $(J - K, J)$  diagram are good multiple system candidates. The study of the binary frequency across the magnitude range probed by our survey would shed light on the the possible population of wide low-mass binaries in Upper Sco recently claimed by Bouy et al. (2006).

Visual inspection of the images revealed two close systems, USco J161520.1–233355 and USco J161336.9–232730 separated by 5.08 and 7.92 arcsec, respectively. Unfortunately our proper motion accuracy is not sufficient to make any firm statement as to the physical association of either of these potential wide binaries, but if confirmed as physical binary members of Upper Sco, either system would be a wide low-mass ( $\sim 0.2 M_{\odot}$ ) binary with a separation of  $\sim 1000$  AU. Other wide low-mass binaries have recently been reported by Bouy et al. (2006) and Luhman (2005). This type of binary is important to studies investigating the formation of low-mass stars and brown dwarfs in open clusters as well as their evolution with time.

## 4.3 The IMF in Upper Sco

We considered the 129 candidates selected in the 6.5 square degree area surveyed in Upper Sco to derive the mass function. We have transformed the  $J$  magnitudes into masses using the NextGen models for masses above  $0.05 M_{\odot}$  and DUSTY isochrones below (Baraffe et al. 1998; Chabrier et al. 2000). The number of candidates per unit of mass ( $dN/dM$ ) was obtained by dividing the number of

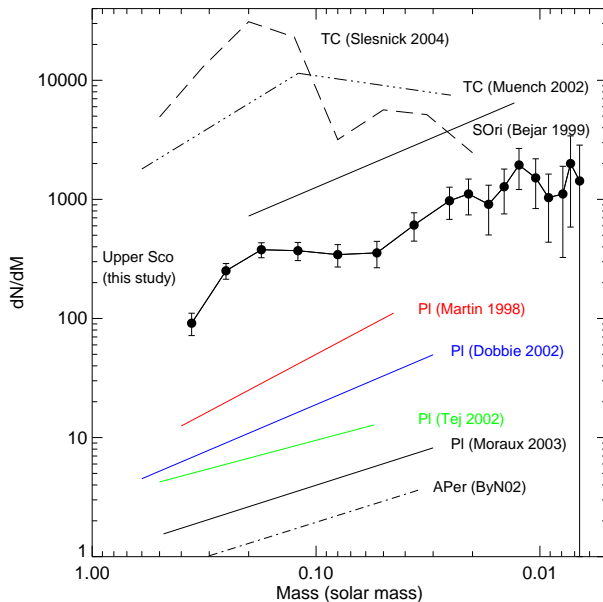


**Figure 9.** Cluster Initial Mass Functions for the Upper Sco association using the members selected from their photometry. We have employed three methods to derive the Upper Sco mass function: open triangles represent a two-fold increase in mass, starting with the 5–10 Jupiter masses bin. Open squares symbolise the mass function drawn from the number of sources in 1.5 magnitude bins. Finally, filled circles correspond to a “smoothed” mass function by counting the number of objects per magnitude bin by steps of 0.5 magnitudes. Overplotted are mass functions from the literature for the Pleiades (Martín et al. 1998; Tej et al. 2002; Dobbie et al. 2002; Moraux et al. 2003),  $\alpha$  Per (Barrado y Navascués et al. 2002),  $\sigma$  Orionis (Béjar et al. 2001), and the Trapezium Cluster (Muench et al. 2002; Slesnick et al. 2004).

objects in each magnitude bin ( $dN$ ) by the difference of the upper and lower limits of the bin in mass ( $M_2 - M_1$ ). We have derived the IMF, expressed as the mass spectrum ( $dN/dM \propto M^\alpha$ ), using 3 approaches (we did not correct for binaries):

- (i) We counted the number of objects per mass bin starting at 5–10 Jupiter masses and increased it two-fold every time (open triangles in Fig. 9).
- (ii) We summed the number of candidates per 1.5 magnitude bin from  $J = 11.5$  mag (open squares in Fig. 9).
- (iii) We made a “smoothed” mass function by counting the number of candidates per magnitude bin by steps of 0.5 magnitudes, starting at  $J = 10.5$ – $11.5$  mag (filled circles in Fig. 9).

The higher mass bin is likely incomplete due to our saturation limit occurring at  $J = 10.5$  mag, corresponding to  $M = 0.48 M_{\odot}$ . Similarly, the lower mass bins below  $0.01 M_{\odot}$  represent lower limits because our survey is limited by the  $Y$  completeness ( $Y = 19.8$  mag or  $M \sim 0.01 M_{\odot}$ ). The best fit of the mass spectrum in Upper Sco is obtained for a single segment of power law index  $\alpha = 0.6 \pm 0.1$  over the  $0.3$ – $0.01 M_{\odot}$  mass range. The mass function is approximately linear across the entire mass spectrum probed by our study (Fig. 9) and in agreement with esti-

mated IMF for the Pleiades ( $\alpha = 0.6\text{--}1.0$ ; Martín et al. 1998; Tej et al. 2002; Dobbie et al. 2002; Moraux et al. 2003),  $\alpha$  Per ( $0.59\pm 0.05$ ; Barrado y Navascués et al. 2002), and  $\sigma$  Orionis ( $0.8\pm 0.4$ ; Béjar et al. 2001). Optical surveys in open clusters derived contamination level on the order of 30–45% (Barrado y Navascués et al. 2002), even in proper motion samples (Moraux et al. 2001). We expect our sample of candidates to be less affected by contaminants as very few sources were detected to the right of our selection criteria in a control field towards the open cluster IC4665. Indeed, the gap between the association sequence and field stars is large, particularly at fainter magnitudes. Spectroscopic follow-up will nevertheless be required to verify the low level of contamination in order to check our mass function in the low-mass and substellar regimes.

Finally, we compare the mass functions of Upper Sco and the Trapezium Cluster in Fig. 9. Muench et al. (2002) modelled the IMF from a near-infrared survey of the Orion region. More recently, Slesnick et al. (2004) obtained optical and infrared spectra of candidates in the inner region of the Trapezium Cluster, yielding mass and extinction for each individual source. The Trapezium Cluster appears to have a break at about  $0.1 M_{\odot}$ , suggesting a lower number of brown dwarfs compared to low-mass stars in contrast to our survey in Upper Sco. If real, this effect could be explained by the continuous formation of brown dwarfs with time up to 5 Myr and perhaps beyond. There is no evidence for this hypothesis in theoretical simulations (Bate & Bonnell 2005; Jappsen et al. 2005). Photo-evaporation of low-mass stars could be playing some role in the Trapezium Cluster although very unlikely (Kroupa & Bouvier 2003). The inner region of the Trapezium Cluster might also have suffered from dynamical ejection of the lowest mass members due to the O stars. The reason for the discrepancy in the mass functions remains unclear but it is too early to claim any difference due to the uncertainties in the pre-main sequence tracks at such early ages (Baraffe et al. 2002).

## 5 CONCLUSIONS

We have presented a deep near-infrared survey in the Upper Sco association conducted during the Science Verification phase of the UKIDSS Galactic Cluster Survey. The survey is complete down to  $Z = 20.1$  mag, corresponding to  $0.01 M_{\odot}$ , and is 3 magnitudes deeper than any previous study in the region. We have confirmed the photometric membership of 129 candidates in the  $0.3\text{--}0.007 M_{\odot}$  mass range. Among them, 116 have proper motion consistent with the mean motion of the association. We have discovered a dozen new brown dwarf candidates below 15 Jupiter masses, according to theoretical isochrones at 5 Myr. Finally, we have derived the mass spectrum across the stellar/substellar regime, yielding a power law with a slope  $\alpha$  of  $0.6\pm 0.1$ , consistent with previous studies in open clusters.

We have demonstrated the power of the UKIDSS Galactic Cluster Survey to select genuine cluster members in a young open cluster from the photometry in 5 passbands as well as the proper motion by using 2MASS as first epoch. This result is extremely promising for the remaining open clusters and star-forming regions targeted by the GCS, including the Pleiades and  $\alpha$  Per. The second epoch conducted

in the  $K$  band within the framework of the GCS will provide complete samples of very low-mass stars and brown dwarfs over the entire cluster with photometric and proper motion membership.

## ACKNOWLEDGMENTS

NL and TRK are postdoctoral research associates funded by the UK PPARC. We are grateful to Isabelle Baraffe and France Allard for providing us with the NextGen, DUSTY and COND models for the WFCAM filters. We acknowledge Matthew Bate and Pavel Kroupa for discussion on the mass function. We thank our colleagues at the UK Astronomy Technology Centre, the Joint Astronomy Centre in Hawaii, the Cambridge Astronomical Survey and Edinburgh Wide Field Astronomy Units for building and operating WFCAM and its associated data flow system. The authors wish to extend special thanks to those of Hawaiian ancestry on whose sacred mountain we are privileged to be guests. This research has made use of the Simbad database, operated at the Centre de Données Astronomiques de Strasbourg (CDS), and of NASA's Astrophysics Data System Bibliographic Services (ADS). This publication has also made use of data products from the Two Micron All Sky Survey, which is a joint project of the University of Massachusetts and the Infrared Processing and Analysis Center/California Institute of Technology, funded by the National Aeronautics and Space Administration and the National Science Foundation.

## REFERENCES

- Ardila D., Martín E., Basri G., 2000, *AJ*, 120, 479  
 Béjar V. J. S., Martín E. L., Zapatero Osorio M. R., Rebolo R., Barrado y Navascués D., Bailer-Jones C. A. L., Mundt R., Baraffe I., Chabrier C., Allard F., 2001, *ApJ*, 556, 830  
 Baraffe I., Chabrier G., Allard F., Hauschildt P. H., 1998, *A&A*, 337, 403  
 Baraffe I., Chabrier G., Allard F., Hauschildt P. H., 2002, *A&A*, 382, 563  
 Barrado y Navascués D., Bouvier J., Stauffer J. R., Lodieu N., McCaughrean M. J., 2002, *A&A*, 395, 813  
 Barrado y Navascués D., Stauffer J. R., Briceño C., Patten B., Hambly N. C., Adams J. D., 2001, *ApJS*, 134, 103  
 Bate M. R., Bonnell I. A., 2005, *MNRAS*, 356, 1201  
 Bouy H., Martín E. L., Brandner W., Zapatero-Osorio M. R., Béjar V. J. S., Schirmer M., Huéramo N., Ghez A. M., 2006, *A&A*, 451, 177  
 Chabrier G., Baraffe I., Allard F., Hauschildt P., 2000, *ApJ*, 542, 464  
 Cutri R. M., Skrutskie M. F., van Dyk S., Beichman C. A., Carpenter J. M., Chester T., Cambresy L., Evans T., Fowler J., Gizis J., 15 coauthors 2003, 2MASS All Sky Catalog of point sources, 2246  
 de Bruijne J. H. J., Hoogerwerf R., Brown A. G. A., Aguilar L. A., de Zeeuw P. T., 1997, in *ESA SP-402: Hipparcos - Venice '97 Improved Methods for Identifying Moving Groups*. pp 575–578  
 de Zeeuw P. T., Hoogerwerf R., de Bruijne J. H. J., Brown A. G. A., Blaauw A., 1999, *AJ*, 117, 354

- Dobbie P. D., Kenyon F., Jameson R. F., Hodgkin S. T., Pinfield D. J., Osborne S. L., 2002, MNRAS, 335, 687
- Dobbie P. D., Pinfield D. J., Jameson R. F., Hodgkin S. T., 2002, MNRAS, 335, L79
- Dye S., Warren S. J., Hambly N. C., Cross N. J. G., Hodgkin S. T., Irwin M. J., Lawrence A., Adamson A. J., Almaini O., Edge A. C., Hirst P., Jameson R. F., Lucas P. W., co-authors. , 2006, astro-ph/0603608
- Hewett P. C., Warren S. J., Leggett S. K., Hodgkin S. T., 2006, MNRAS, 367, 454
- Jappsen A.-K., Klessen R. S., Larson R. B., Li Y., Mac Low M.-M., 2005, A&A, 435, 611
- Kroupa P., 2002, Science, 295, 82
- Kroupa P., Bouvier J., 2003, MNRAS, 346, 343
- Lawrence A., Warren S. J., Almaini O., Edge A. C., Hambly N. C., Jameson R. F., co-authors. , 2006, arXiv:astro-ph/0604426
- Leggett S. K., 1992, ApJS, 82, 351
- Luhman K. L., 2005, ApJL, 633, L41
- Martín E. L., Delfosse X., Guieu S., 2004, AJ, 127, 449
- Martín E. L., Zapatero Osorio M. R., Rebolo R., 1998, in ASP Conf. Ser. 134: “Brown Dwarfs and Extrasolar Planets”, eds. R. Rebolo, E. L. Martín, and M. R. Zapatero Osorio The Substellar Initial Mass Function in the Pleiades. p. p 507
- McGovern M. R., Kirkpatrick J. D., McLean I. S., Burgasser A. J., Prato L., Lowrance P. J., 2004, ApJ, 600, 1020
- Mohanty S., Basri G., Jayawardhana R., Allard F., Hauschildt P., Ardila D., 2004, ApJ, 609, 854
- Mohanty S., Jayawardhana R., Basri G., 2004, ApJ, 609, 885
- Moralex E., Bouvier J., Stauffer J. R., 2001, A&A, 367, 211
- Moralex E., Bouvier J., Stauffer J. R., Cuillandre J.-C., 2003, A&A, 400, 891
- Muench A. A., Lada E. A., Lada C. J., Alves J., 2002, ApJ, 573, 366
- Preibisch T., Guenther E., Zinnecker H., 2001, AJ, 121, 1040
- Preibisch T., Guenther E., Zinnecker H., Sterzik M., Frink S., Roeser S., 1998, A&A, 333, 619
- Preibisch T., Zinnecker H., 2002, AJ, 123, 1613
- Scalo J., 1998, in ASP Conf. Ser. 142: The Stellar Initial Mass Function (38th Herstmonceux Conference) The IMF Revisited: A Case for Variations. p. 201
- Slesnick C. L., Carpenter J. M., Hillenbrand L. A., 2006, AJ, 131, 3016
- Slesnick C. L., Hillenbrand L. A., Carpenter J. M., 2004, ApJ, 610, 1045
- Tej A., Sahu K. C., Chandrasekhar T., Ashok N. M., 2002, ApJ, 578, 523
- Walter F. M., Vrba F. J., Mathieu R. D., Brown A., Myers P. C., 1994, AJ, 107, 692
- Zapatero Osorio M. R., Rebolo R., Martín E. L., 1997, A&A, 317, 164

(UKIDSSR2) held at the WFCAM Science Archive. The SQL query given in the Appendix was used to create Fig. 3.

Comments in the script indicate the various selection cuts made. Note that in the **SELECT** statement we explicitly compute colours based on aperture magnitudes optimal for point sources. In all database releases after science verification this is not necessary as these colours are held by default in the merged source tables as **zmyPnt** etc. (the science verification data had colours based on the larger Hall radius aperture magnitudes). Also, the sample selection requires that candidates be detected in YJHK bands, but to push the sample selection fainter and redder we are careful to allow default values of the *Z* photometric attributes to retain stars not detected in that passband. Furthermore, we employ morphological classification codes  $-1$  (stellar) and  $-2$  (possibly stellar) to maximise completeness. Finally, the **WHERE** predicate (**priOrSec=0 OR priOrSec=frameSetID**) purges secondary duplicates in overlap regions. For more details concerning the use of SQL and data in the WFCAM Science Archive, see Hambly et al. (2006) and references therein.

## APPENDIX B: TABLE OF PHOTOMETRIC NON-MEMBERS

## APPENDIX C: TABLE OF PROPER MOTION NON-MEMBERS

## APPENDIX A: SQL QUERY SUBMITTED TO THE WFCAM SCIENCE ARCHIVE

Initial sample selection for this Upper Sco study was made by accessing the UKIDSS Science Verification database

```

SELECT
/* Attribute selection: */
g.ra, g.dec, zaperMag3-yaperMag3 AS zmy, zaperMag3-japerMag3 AS zmj,
zaperMag3-k_1aperMag3 AS zmk, yaperMag3-japerMag3 AS ymj,
japerMag3-haperMag3 AS jmh, haperMag3-k_1aperMag3 AS hmk,
japerMag3-k_1aperMag3 AS jmk, zaperMag3, yaperMag3,
japerMag3, haperMag3, k_1aperMag3, zaperMag3Err, yaperMag3Err,
japerMag3Err, haperMag3Err, k_1aperMag3Err

FROM
/* Table(s) from which to select the attributes: */
gcsSource as g

WHERE
/* Sample selection predicates:
only Upper Sco data (no other GCS target is south of the equator) */
g.dec < 0.0
/* Bright saturation cut-offs */
AND (zaperMag3 < -0.9e9 OR zaperMag3 > 11.4)
AND yaperMag3 > 11.3
AND japerMag3 > 10.5
AND haperMag3 > 10.2
AND k_1aperMag3 > 9.7
/* Limit merged passband selection to +/- 1 arcsec */
AND (zXi BETWEEN -1.0 AND +1.0 OR zXi < -0.9e9)
AND yXi BETWEEN -1.0 AND +1.0
AND jXi BETWEEN -1.0 AND +1.0
AND hXi BETWEEN -1.0 AND +1.0
AND k_1Xi BETWEEN -1.0 AND +1.0
AND (zEta BETWEEN -1.0 AND +1.0 OR zEta < -0.9e9)
AND yEta BETWEEN -1.0 AND +1.0
AND jEta BETWEEN -1.0 AND +1.0
AND hEta BETWEEN -1.0 AND +1.0
AND k_1Eta BETWEEN -1.0 AND +1.0
/* Retain only point-like sources */
AND (zClass BETWEEN -2 AND -1 OR zClass = -9999)
AND yClass BETWEEN -2 AND -1
AND jClass BETWEEN -2 AND -1
AND hClass BETWEEN -2 AND -1
AND k_1Class BETWEEN -2 AND -1
/* Retain only the best record when duplicated in an overlap region */
AND (priOrSec = 0 OR priOrSec = g.frameSetID)

```

In order to get proper motion information, substitute the following for the FROM clause above:

```

gcsMergeLog AS l, Multiframe AS mj, (
  SELECT t.ra AS ra, t.dec AS dec, x.slaveObjID AS slaveObjID,
         x.masterObjID as masterObjID, t.j_m, t.h_m, t.k_m, t.jdate
  FROM   gcsSourceXtwomass_psc as x, TWOMASS..twomass_psc as t
  WHERE  x.slaveObjID=t.pts_key AND distanceMins IN (
         SELECT MIN(distanceMins) FROM gcsSourceXtwomass_psc WHERE masterObjID=x.masterObjID
         )
) AS T2 RIGHT OUTER JOIN gcsSource AS g ON (g.sourceID=T2.masterObjID)

```

along with the following additional WHERE predicates:

```

AND g.frameSetID=l.frameSetID
AND l.jmfID=mj.multiframeID

```

and the following two additional SELECTIONS to obtain relative proper motions with respect to 2MASS in units of milliarcsec yr<sup>-1</sup>:

```

3.6e6*COS(RADIANS(g.dec))*(g.ra-T2.ra)/((mj.mjdObs - T2.jdate+2400000.5)/365.25) AS pmRA,
3.6e6*(g.dec-T2.dec)/((mj.mjdObs - T2.jdate+2400000.5)/365.25) AS pmDEC

```

**Figure A1.** Structured Query Language (SQL) query used on the WFCAM Science Archive database UKIDSSR2 to select the GCS Upper Sco sample discussed in the paper. The query returns 133,476 rows of data.

**Table B1.** Coordinates (J2000), *ZYJHK* photometry, and proper motions of 18 photometric non-members (open squares in the colour-magnitude and colour-colour diagrams).

R.A.	Dec.	<i>Z</i>	<i>Y</i>	<i>J</i>	<i>H</i>	<i>K</i>	$\mu_\alpha \cos \delta$	$\mu_\delta$
16 06 30.92	-22 58 15.2	16.658±0.011	15.990±0.008	14.985±0.004	13.628±0.003	12.414±0.002	99.9	99.9
16 07 03.05	-23 31 46.2	12.024±0.001	11.539±0.001	10.982±0.001	10.393±0.000	9.792±0.000	10.2	-24.9
16 07 25.70	-23 14 58.0	20.893±0.398	19.434±0.138	18.790±0.128	17.960±0.111	17.816±0.178	99.9	99.9
16 07 27.57	-21 54 42.7	17.010±0.015	16.198±0.010	15.588±0.007	14.990±0.006	14.564±0.009	99.9	99.9
16 07 29.54	-23 08 22.3	12.815±0.001	12.365±0.001	11.749±0.001	10.970±0.000	10.188±0.000	99.9	99.9
16 08 20.24	-23 33 41.7	20.910±0.387	19.780±0.198	18.689±0.118	18.291±0.148	18.387±0.283	99.9	99.9
16 08 39.70	-23 06 57.8	18.487±0.042	15.984±0.008	15.596±0.007	15.040±0.007	14.889±0.011	99.9	99.9
16 10 51.82	-23 33 26.3	16.359±0.009	15.581±0.006	14.969±0.005	14.343±0.005	13.985±0.006	-67.9	-110.7
16 11 08.90	-23 08 28.3	11.664±0.001	11.361±0.001	10.783±0.000	10.499±0.000	10.051±0.000	-16.6	-32.0
16 11 24.88	-22 52 53.3	17.715±0.023	16.735±0.016	16.007±0.011	15.315±0.008	14.875±0.011	99.9	99.9
16 12 05.64	-22 24 12.4	19.915±0.157	18.568±0.063	17.546±0.038	16.990±0.033	16.500±0.045	99.9	99.9
16 12 34.14	-21 44 50.2	13.461±0.002	12.831±0.002	12.387±0.001	11.704±0.001	11.205±0.001	-6.0	-26.7
16 13 01.40	-21 42 54.5	18.135±0.035	17.201±0.020	16.325±0.011	15.613±0.010	15.065±0.013	99.9	99.9
16 13 39.04	-22 33 14.4	19.558±0.109	18.399±0.061	17.418±0.042	16.836±0.033	16.227±0.039	99.9	99.9
16 14 50.26	-23 32 39.9	12.758±0.001	12.218±0.001	11.605±0.001	10.803±0.000	10.067±0.000	-18.2	-16.4
16 15 03.04	-23 52 50.3	17.473±0.019	16.650±0.013	15.932±0.009	15.286±0.010	14.842±0.012	99.9	99.9
16 15 27.63	-23 52 34.2	14.833±0.004	13.989±0.003	13.271±0.002	12.442±0.001	11.808±0.001	0.1	-27.6
16 16 22.51	-23 38 42.6	20.331±0.220	18.841±0.080	17.991±0.058	17.247±0.060	16.989±0.083	99.9	99.9

**Table C1.** Coordinates (J2000), *ZYJHK* photometry, and proper motions of 26 proper motion non-members (open diamonds in the colour-magnitude and colour-colour diagrams).

R.A.	Dec.	<i>Z</i>	<i>Y</i>	<i>J</i>	<i>H</i>	<i>K</i>	$\mu_\alpha \cos \delta$	$\mu_\delta$
16 06 57.53	-23 03 27.1	11.759±0.001	11.404±0.001	10.901±0.000	10.341±0.000	9.970±0.000	-11.8	9.7
16 07 03.05	-23 31 46.2	12.024±0.001	11.539±0.001	10.982±0.001	10.393±0.000	9.792±0.000	10.2	-24.9
16 07 27.57	-21 54 42.7	17.010±0.015	16.198±0.010	15.588±0.007	14.990±0.006	14.564±0.009	-83.1	-51.3
16 07 48.27	-21 39 03.9	13.962±0.002	13.300±0.002	12.686±0.001	12.118±0.001	11.778±0.001	-2.8	-4.5
16 08 27.33	-22 17 29.3	12.756±0.001	12.183±0.001	11.630±0.001	10.991±0.000	10.586±0.001	0.4	-8.1
16 08 28.69	-21 37 20.0	12.758±0.001	12.154±0.001	11.598±0.001	11.073±0.000	10.685±0.001	-31.4	-20.5
16 08 34.55	-22 11 55.9	13.772±0.002	13.067±0.002	12.500±0.001	11.943±0.001	11.556±0.001	-7.1	-5.2
16 09 05.67	-22 45 16.7	17.341±0.019	16.049±0.008	15.212±0.006	14.558±0.006	13.987±0.007	-25.7	-9.9
16 09 07.75	-23 39 54.5	13.438±0.002	12.629±0.001	12.032±0.001	11.476±0.001	11.107±0.001	-17.1	-3.7
16 09 08.83	-22 17 46.9	14.124±0.003	13.466±0.002	12.903±0.001	12.403±0.001	12.046±0.001	-36.5	-29.6
16 09 32.29	-22 29 36.0	12.421±0.001	11.930±0.001	11.383±0.001	10.764±0.000	10.445±0.001	-6.1	8.2
16 09 37.85	-21 23 19.0	12.638±0.001	12.170±0.001	11.700±0.001	11.187±0.001	10.877±0.001	-3.6	-241.2
16 10 00.18	-23 12 19.3	15.947±0.007	15.204±0.005	14.530±0.004	13.977±0.004	13.545±0.004	-33.5	-14.2
16 10 02.67	-23 44 39.5	12.413±0.001	11.758±0.001	11.204±0.001	10.682±0.000	10.265±0.001	-177.8	89.7
16 10 02.86	-23 44 40.9	11.900±0.001	11.395±0.001	10.862±0.000	10.427±0.000	9.949±0.000	252.5	-145.7
16 10 19.43	-23 31 08.9	14.842±0.004	14.123±0.003	13.532±0.002	12.967±0.002	12.571±0.002	-5.1	-2.5
16 10 51.82	-23 33 26.3	16.359±0.009	15.581±0.006	14.969±0.005	14.343±0.005	13.985±0.006	-67.9	-110.7
16 14 01.73	-22 58 48.7	13.654±0.002	12.981±0.002	12.422±0.001	11.882±0.001	11.515±0.001	312.7	-410.9
16 14 12.36	-22 19 13.2	12.469±0.001	11.982±0.001	11.446±0.001	11.057±0.000	10.568±0.001	8.8	0.2
16 14 25.25	-23 50 15.1	13.520±0.002	12.875±0.001	12.341±0.001	11.804±0.001	11.422±0.001	-14.2	-5.0
16 14 46.84	-23 41 57.2	16.314±0.009	15.494±0.006	14.835±0.004	14.251±0.004	13.815±0.005	-34.6	-14.9
16 15 16.02	-23 45 10.4	13.587±0.002	12.844±0.001	12.230±0.001	11.656±0.001	11.272±0.001	-11.0	3.9
16 15 16.66	-23 40 46.3	17.968±0.030	16.552±0.013	15.621±0.008	14.911±0.007	14.269±0.008	-35.1	-11.1
16 15 38.43	-23 41 56.0	13.399±0.002	12.760±0.001	12.208±0.001	11.584±0.001	11.267±0.001	-32.1	-16.2
16 16 20.11	-23 44 14.3	12.083±0.001	11.504±0.001	10.976±0.001	10.533±0.000	10.144±0.000	-33.2	-11.3
16 16 26.20	-23 50 48.8	12.051±0.001	11.601±0.001	11.018±0.001	10.474±0.000	9.968±0.000	-10.0	1.1